

Single and Multiple Lewis Sites of MgO: A Combined IR and *ab Initio* Study with CD₃CN as a Molecular Probe

A. G. Pel'menschikov,^{*,†} G. Morosi, and A. Gamba

Dipartimento di Chimica Fisica ed Elettrochimica, Università' di Milano-Sede di Como, Via Lucini 3, 22100 Como, Italy

S. Coluccia,[‡] G. Martra,[‡] and E. A. Paukshtis[§]

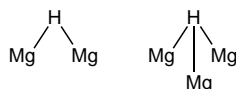
Dipartimento di Chimica Inorganica, Chimica Fisica e Chimica dei Materiali, Università' di Torino, Via P. Giuria 7, 10125 Torino, Italy, and Borekov Institute of Catalysis, Prosp. Lavrentieva 5, 630090 Novosibirsk, Russia

Received: September 15, 1995[®]

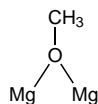
CD₃CN is used for the first time for characterizing Lewis sites of MgO ex-hydroxide in a combined IR and *ab initio* study. Four $\nu(\text{CN})$ bands of coordinated CD₃CN species are observed at 2317, 2302, 2293, and 2280 cm⁻¹ at low coverages. The 2302 and 2293 cm⁻¹ bands are attributed to CD₃CN on Mg_{3c} and Mg_{4c} sites at the intersections of regular MgO faces of the (001) type. The 2317 and 2280 cm⁻¹ bands are assigned to CD₃CN stabilized by two neighboring Mg_{4c} sites on (110) defect faces and by two neighboring Mg_{3c} sites at the intersections of the (001) and (110) faces, respectively. This assignment is supported by the theoretical reproduction of the experimental $\Delta\nu(\text{CN})$ shifts to an accuracy of a few cm⁻¹. The only other detected $\nu(\text{CN})$ band, which appears at high coverages, is the $\nu(\text{CN}) = 2261$ cm⁻¹ band of liquid CD₃CN. This fact and results of frequency and energy analyses suggest the energy of CD₃CN adsorption on Mg_{5c} sites of the (001) faces to be smaller than the energy of CD₃CN liquefaction.

Introduction

IR spectroscopic investigations using probe molecules^{1–7} postulate the existence of some multiple Mg sites on MgO, besides the generally discussed three-coordinated Mg_{3c}, four-coordinated Mg_{4c}, and five-coordinated Mg_{5c} single sites of the idealized rock-salt structure microcrystals.^{8–14} Being very active, these sites have raised significant interest (refs 1–7 and references therein), as they could play an important role in many chemical processes on MgO. Two hypothetical structures of the multiple sites have been suggested in IR studies. As Coluccia et al. inferred^{2,7} from an analogy between IR features of H species on MgO, CaO, and SrO and on MgH₂, CaH₂, and SrH₂, one of the most typical broad bands of chemisorbed hydrogen species on MgO ex-hydroxide, namely the 1130 cm⁻¹ band, should be attributed to Mg₂H or Mg₃H bridge structures



Strengthening this conclusion, Bensitel et al.⁶ proposed that one of the main chemisorbed forms of CH₃OH on MgO ex-hydroxide, MgO ex-carbonate, and MgO smoke, which manifests itself by the $\nu(\text{CO})$ band at 1090 cm⁻¹, is a Mg₂OCH₃ bridge methoxy group



As suggested in these studies (see also ref 5), the most likely adsorbing sites involved in these bridge structures are double-Mg_{4c} and triple-Mg_{3c} sites



of (110) and (111) defect microplanes. In our present study an attempt is undertaken to define exactly the structure of multiple Mg sites of MgO ex-hydroxide by the quantum chemical analysis of the experimental $\Delta\nu(\text{CN})$ frequency shifts of CD₃CN on this oxide. The $\Delta\nu(\text{CN})$ shifts of CD₃CN on Mg_{3c}, Mg_{4c}, and Mg_{5c} sites are also calculated to distinguish between the $\nu(\text{CN})$ bands of CD₃CN species on the single and multiple Mg sites in the spectra.

Acetonitrile is known to be a very efficient probe for IR spectroscopic characterization of Brønsted and Lewis sites of oxides.^{15–20} Starting from the pioneering IR studies on CH₃CN adducts by Filimonov et al.,^{21,22} this use of the molecule is based on a well-pronounced dependence of its $\nu(\text{CN})$ frequency on the strength of the electron-donor interaction through the nitrogen lone pair in series of closely related Lewis acids; a strengthening of the interaction leads to an upward shift of the frequency. As Filimonov et al. suggested²² and Purcell and Drago confirmed later^{20,23,24} by vibrational and Mulliken overlap population analyses, this effect is caused by the stabilization of the CN σ orbital upon electron donation from the nitrogen lone pair. CD₃CN is a more convenient probe than CH₃CN as the interpretation of the CH₃CN $\Delta\nu(\text{CN})$ shift is strongly complicated by the Fermi resonance between the $\nu(\text{CN})$ and $\delta_s(\text{CH}_3) + \nu(\text{CC})$ levels.^{18,19,25} In SCF/3-21G calculations¹⁹ by Pel'menschikov et al., the experimental $\Delta\nu(\text{CN})$ shifts of CD₃CN

[†] Present address: Università' di Milano-Sede di Como, Via Lucini 3, 22100 Como, Italy.

[‡] Università' di Torino.

[§] Borekov Institute of Catalysis.

[®] Abstract published in *Advance ACS Abstracts*, February 15, 1996.

on $\equiv\text{Si}-\text{OH}$, $\equiv\text{Si}-\text{O}(\text{H})\cdot\text{Al}\equiv$, and low- and high-coordinated Lewis Al sites of zeolites were reproduced to an accuracy of 5 cm^{-1} using $\text{Si}(\text{OH})_4$, $(\text{HO})_3\text{SiOHAl}(\text{OH})_3$, $\text{Al}(\text{OH})_3$, and $\text{Al}(\text{OH})_3\cdot 2\text{H}_2\text{O}$ molecular models of the sites. In more recent SCF/6-31G* calculations, Pel'menschikov et al.²⁶ reproduced within a few cm^{-1} also the $\Delta\nu(\text{CO})$ shifts of CO on Mg_{3c} and Mg_{4c} sites of MgO using Mg_4O_4 and Mg_6O_6 molecular models. Both these results suggest that the molecular quantum chemical modeling might give a significant strength to the further use of CD_3CN as an IR probe of oxides through the theoretical check of hypothetical CD_3CN surface structures against experimental IR data. These considerations prompted us to conduct a joint IR and quantum chemical study of the structure of multiple Mg sites of MgO ex-hydroxide using a CD_3CN probe.

In this investigation, like in refs 27–31, we take advantage of the synergetic effect in identifying unknown adsorption species that arises from the combined use of experimental IR and computational quantum chemical methods.

Experimental Section

MgO was prepared by thermal decomposition of $\text{Mg}(\text{OH})_2$ at $\sim 540\text{ K}$ in the IR cell.⁴ Prior to CD_3CN adsorption, the pellet was outgassed at 1123 K . The final surface area was $\sim 200\text{ m}^2\text{ g}^{-1}$.

IR spectra were obtained by a Bruker IFS 48 instrument at room temperature. The resolution was 4 cm^{-1} . The IR cell was permanently connected to a standard vacuum system and allowed all thermal pretreatments and adsorption–desorption experiments to be carried out *in situ*.

Details of Calculations

Ab initio SCF calculations were performed using the GAUSSIAN-92 package.³² In adsorption complexes the geometry of CD_3CN and its position with respect to MgO models were fully optimized within adopted symmetry constraints. In the MgO models only the position of the adsorbing Mg atom was optimized, while the positions of all the other Mg and O atoms correspond to those in magnesium oxide ($R_{\text{MgO}} = 2.1\text{ \AA}$). This is in line with the generally accepted methodology of the molecular modeling for ionic oxides.^{8–14,26} The optimized geometries can be obtained from the authors on request.

The stability of the calculated binding energies with respect to the basis set superposition error (BSSE) was checked by the counterpoise method.³³

Results and Discussion

1. IR Experiments. Figure 1A shows the changes in the $2340\text{--}2250\text{ cm}^{-1}$ spectral region of the $\nu(\text{CN})$ band upon the admission of successive small doses of CD_3CN . Two CN bands appear at 2317 and 2293 cm^{-1} at very low coverages (Figure 1A, spectra a and b). The upward shifts of these bands with respect to the $\nu(\text{CN}) = 2272\text{ cm}^{-1}$ frequency of the free CD_3CN ¹⁹ indicate that the related CD_3CN molecules are coordinated on some electron-acceptor sites through the nitrogen lone pair. As the adsorption proceeds, the 2317 cm^{-1} band fades away (Figure 1A, spectra c and d). Unlike the 2293 cm^{-1} band, this band does not reappear upon repeated CD_3CN adsorption after prolonged outgassing of the loaded sample. This means that the coordination on the corresponding Mg sites is followed by some irreversible chemical transformation deactivating these sites. This conclusion agrees with the emergence of few very intense IR bands of chemisorbed species in the $2200\text{--}1440\text{ cm}^{-1}$ spectral region (the spectrum is not reported), which are not affected by evacuation. The mechanism of this reaction will

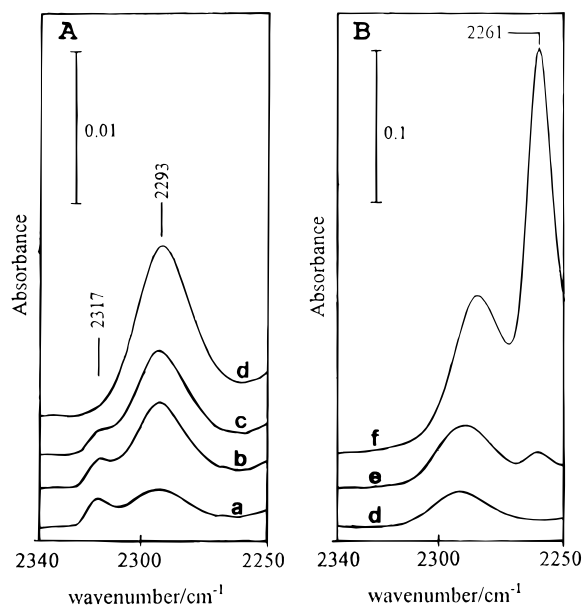


Figure 1. Infrared spectra of CD_3CN adsorbed on MgO ex-hydroxide: (A) a–d, after the admission of successive small doses of CD_3CN and (B) e–f, in the presence of excess CD_3CN at the residual pressures of 3 and 20 mbar, respectively.

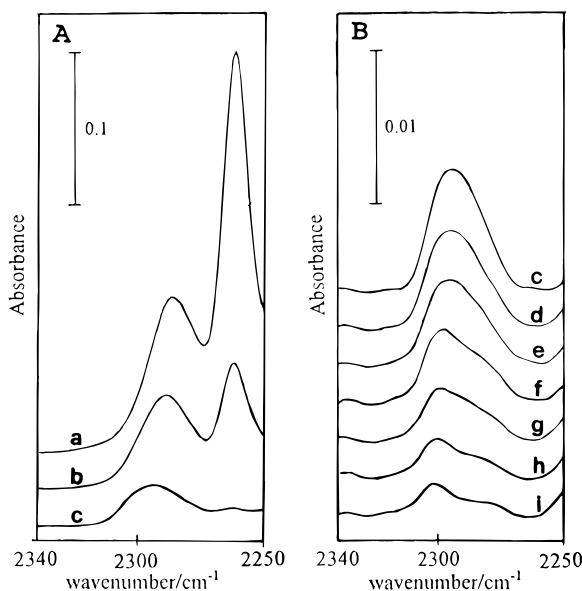


Figure 2. Infrared spectra of CD_3CN adsorbed on MgO ex-hydroxide: (A) under progressively reduced pressure from 20 (a) to 0.05 mbar (e) and (B) after further outgassing for 20 s (f), 1 min (g), 2 min (h), and 15 min (i).

be discussed in a separate report.³⁴ The only additional band emerging in the $2340\text{--}2250\text{ cm}^{-1}$ region upon admission of the excess CD_3CN doses, up to the pressure of 20 mbar, is the $\nu(\text{CN}) = 2261\text{ cm}^{-1}$ band of liquid CD_3CN ¹⁸ (Figure 1B).

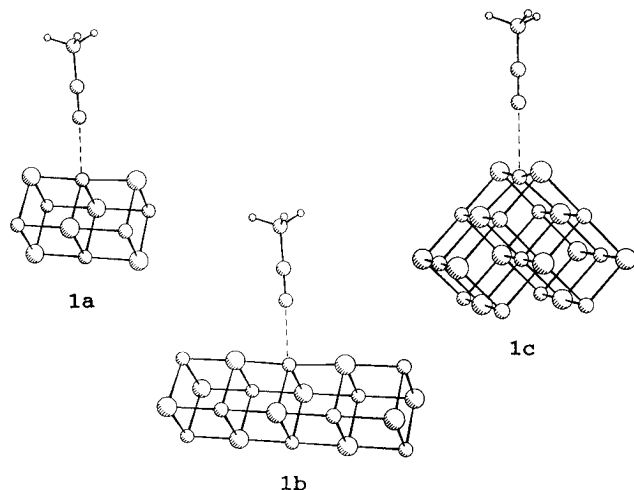
Figure 2 shows the behavior of the 2293 and 2261 cm^{-1} bands upon progressive outgassing of the preadsorbed CD_3CN . The 2261 cm^{-1} band fades away rapidly, while the 2293 cm^{-1} band diminishes more slowly and successively shifts to the higher frequencies, showing its more complex nature (Figure 2A). The main component of this complex band at $\sim 2293\text{ cm}^{-1}$ disappears first, making evident two other components at 2302 and 2280 cm^{-1} (Figure 2B). These two components should be associated with some strongly bonded CD_3CN species, as they are hardly influenced by further pumping for 1 h.

An interpretation of these IR features will be suggested below on the basis of the results of quantum chemical calculations.

TABLE 1: $\Delta\nu(\text{CN})$ Shift of CD_3CN on the Mg_{4c} Site (cm^{-1})

model	basis set	$\Delta\nu(\text{CN})^a$
$\text{CD}_3\text{CN}\cdot\text{Mg}_6\text{O}_6$ (1a)	6-31G*	24
	CBS1	25
	CBS2	22
$\text{CD}_3\text{CN}\cdot\text{Mg}_{10}\text{O}_{10}$ (1b)	CBS1	20
$\text{CD}_3\text{CN}\cdot\text{Mg}_{12}\text{O}_{12}$ (1c)	CBS2	22

^a With respect to free CD_3CN $\nu(\text{CN}) = 2623 \text{ cm}^{-1}$.

**Figure 3.** Molecular models of CD_3CN on the Mg_{4c} site.

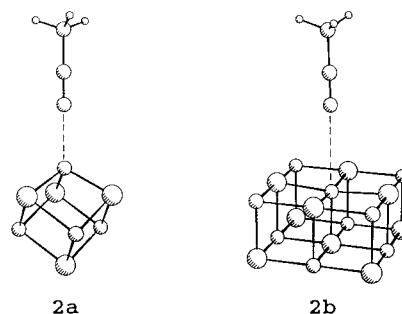
2. Quantum Chemical Calculations. 2.1. Cluster Size and Basis Set Convergencies. As found in ref 26, the $\Delta\nu(\text{CN})$ and $\Delta\nu(\text{CO})$ shifts of CD_3CN and CO on oxides are mainly defined by their very local interactions with the adsorbing sites. As an important practical corollary of this conclusion, the results of the $\Delta\nu(\text{CN})$ and $\Delta\nu(\text{CO})$ computations using molecular models should insignificantly depend both on the model size and on the quantum chemical description out of “the center of cluster”, i.e., the cluster part which is not involved directly in the adsorption interaction. For a further illustration of this point, in Table 1 we report the $\nu(\text{CN})$ shift of CD_3CN on Mg_{4c} sites calculated with $\text{CD}_3\text{CN}\cdot\text{Mg}_6\text{O}_6$, $\text{CD}_3\text{CN}\cdot\text{Mg}_{10}\text{O}_{10}$, and $\text{CD}_3\text{CN}\cdot\text{Mg}_{12}\text{O}_{12}$ models (Figure 3, models **1a**, **1b**, and **1c**) using the 6-31G* and two combined basis sets: the 6-31G* basis set for CD_3CN and the adsorbing Mg atom and the 3-21G basis set for the rest of the model (CBS1) and the 6-31G* basis set for CD_3CN and the adsorbing Mg atom, the 3-21G basis set for the O atoms surrounding this Mg atom, and the STO-3G basis set for the rest of the model (CBS2). The frequency shift is almost independent both of the quantum chemical description out of the center of cluster (cf. the shifts calculated with the $\text{CD}_3\text{CN}\cdot\text{Mg}_6\text{O}_6$ model using the 6-31G*, CBS1, and CBS2 basis sets) and of the model size (cf. the shifts calculated with $\text{CD}_3\text{CN}\cdot\text{Mg}_6\text{O}_6$ and $\text{CD}_3\text{CN}\cdot\text{Mg}_{10}\text{O}_{10}$ models using the CBS1 basis set and with $\text{CD}_3\text{CN}\cdot\text{Mg}_6\text{O}_6$ and $\text{CD}_3\text{CN}\cdot\text{Mg}_{12}\text{O}_{12}$ models using the CBS2 basis set). In ref 26 the computed $\Delta\nu(\text{CO})$ shifts of CO on MgO also proved to be stable upon a similar simplification of the basis set. Therefore, when calculating the frequencies, we will use CBS1 for Mg_9O_9 and CBS2 for even bigger MgO models to reduce the computational cost.

The comparison of the stabilities of the $\Delta\nu(\text{CN})$ shift and of the E_{bin} binding energy upon the change of the basis set further supports the very local nature of the interactions responsible for the $\Delta\nu(\text{CN})$ shift. Although on going from the CBS1 to the CBS2 basis set the binding energy of CD_3CN on Mg_{4c} sites calculated with $\text{CD}_3\text{CN}\cdot\text{Mg}_6\text{O}_6$ and $\text{CD}_3\text{CN}\cdot\text{Mg}_{12}\text{O}_{12}$ models change so strongly that they become negative (Table 2), the corresponding $\Delta\nu(\text{CN})$ shifts change within a few cm^{-1} only

TABLE 2: Binding Energies (kJ/mol)

adsorbing site	model	basis set	E_{bin}^a	+BSSE ^b
Mg_{3c}	2a	6-31G*	74	64
		6-31G*	18	8
Mg_{4c}	1a	CBS1	18	
		CBS2	-15	
	1b	CBS1	22	
		CBS2	(unstable)	
Mg_{5c}	1c	CBS1	21	
		CBS2	-20	
	2b	6-31G*	(unstable)	
		CBS1	15	-6
double- Mg_{4c}	3a	CBS1	30	
triple- Mg_{3c}	3b	CBS1	157	
double- Mg_{3c}	3c	CBS1	113	

^a $E_{\text{bin}} = E(\text{complex}) - [E(\text{substrate}) + E(\text{adsorbate})]$. ^b BSSE corrected values.

**Figure 4.** Molecular models of CD_3CN on Mg_{3c} (**2a**) and Mg_{5c} (**2b**) sites.**TABLE 3:** $\Delta\nu(\text{CN})$ Frequency Shift of CD_3CN (cm^{-1})

adsorbing site	model	calc ^a	exp ^b
Mg_{3c}	2a	26 ^c	30
Mg_{4c}	1a	24 ^c	21
Mg_{5c}	2b	1 ^d	(not found)
double- Mg_{4c}	3a	42 ^e	45
triple- Mg_{3c}	3b	-26 ^e	(not found)
double- Mg_{3c}	3c	4 ^e	8

^a With respect to free CD_3CN $\nu(\text{CN}) = 2623 \text{ cm}^{-1}$. ^b With respect to free CD_3CN $\nu(\text{CN}) = 2272 \text{ cm}^{-1}$. ^c 6-31G* basis set. ^d CBS1. ^e CBS2.

(Table 1). The negative E_{bin} values can be accounted for only by a very strong overestimate of the electrostatic repulsion of CD_3CN from the surface. This result is not correct from the physical point of view, but it emphasizes that the $\Delta\nu(\text{CN})$ is substantially independent of the long range interactions. Taking into account the strong overestimate of the electrostatic repulsion of CD_3CN from the surface when using the CBS2 basis set, only the 6-31G* and CBS1 binding energies will be considered in discussing the relative stability of coordinated CD_3CN species.

The demonstrated convergence of the calculated $\Delta\nu(\text{CN})$ shifts justifies our choice of molecular models and basis sets. As to the adequacy of the molecular approach itself, in recent 6-31G* calculations using similar molecular models we reproduced experimental $\Delta\nu(\text{CN})$ and $\Delta\nu(\text{CO})$ shifts of nine CD_3CN and CO complexes with Bronsted and Lewis sites of silica, zeolites, aluminophosphates, and MgO to an accuracy of 5 cm^{-1} .²⁶ This allows to consider our $\Delta\nu(\text{CN})$ shift prediction to be accurate to a few cm^{-1} .

2.2. CD_3CN Coordination on Single Mg Sites. The predicted $\Delta\nu(\text{CN}) = 26$ and 24 cm^{-1} shifts of CD_3CN on single Mg_{3c} and Mg_{4c} sites (Figure 4, model **2a**, and Figure 3, model **1a**) are very close to the experimental $\Delta\nu(\text{CN}) = 30$ and 21 cm^{-1} shift of the 2302 and 2293 cm^{-1} bands (Table 3). Therefore, we suggest these $\nu(\text{CN})$ bands to be produced by

CD₃CN on Mg_{3c} and Mg_{4c} sites, respectively. The BSSE corrected $E_{\text{bin}} = 64$ and 8 kJ/mol of CD₃CN on Mg_{3c} and Mg_{4c} sites conforms to the fact that the 2302 cm⁻¹ band is significantly more resistant than the 2293 cm⁻¹ band upon outgassing (Figure 2B). The 2293 cm⁻¹ band is much more intense than the 2302 band, in agreement with the similar intensity ratio of the $\nu(\text{CO}) = 2159$ cm⁻¹ and $\nu(\text{CO}) = 2202$ cm⁻¹ bands of CO on the related sites of MgO ex-hydroxide;⁴ this feature suggests that the concentration of Mg_{3c} sites is substantially smaller than the concentration of Mg_{4c} sites.

According to our calculations (Table 3), the $\nu(\text{CN})$ frequency of CD₃CN on Mg_{5c} sites (Figure 4, model **2b**) should marginally differ from the 2272 cm⁻¹ frequency of the free CD₃CN. However, no CN band was detected at frequencies lower than the 2293 cm⁻¹ band besides the 2261 cm⁻¹ band of liquid CD₃CN (Figure 1B). On the basis of this result, we conclude that the energy of CD₃CN adsorption on Mg_{5c} sites should be smaller than the energy of CD₃CN liquefaction, making the adsorption on these sites energetically unfavorable. Also, the energy calculations suggest that the energy of adsorption on Mg_{5c} sites should be very small: at the CBS1 level after the BSSE correction, the binding energy of CD₃CN on the Mg_{5c} site of the Mg₉O₉ model becomes negative, and at the 6-31G* level, CD₃CN on this site is essentially unbounded (Table 2). A similar conclusion was drawn by Scaemhorn et al.³⁵ from results of periodic HF calculations for the H₂O adsorption on Mg_{5c} sites; the computed binding energies for different H₂O configurations on the (001) face suggested that as the coverage increases the H₂O molecules should tend to form hydrogen-bonded aggregates rather than wet the surface.

The unusually weak sensitivity of the $\nu(\text{CN})$ frequency to the nature of the adsorbing site when going from Mg_{3c} to Mg_{4c}, the $\nu(\text{CN})$ changing by only 9 cm⁻¹,³⁶ is very interesting from the theoretical point of view and deserves a comment. According to an empirical regularity^{37,38} and to Mulliken overlap population analyses,^{20,37,38} coordination at the more electronegative atom of a multiple chemical bond weakens the π bonds. This is caused by an increase of the polarity of the π bonds due to the electron density shift toward the electron-donor atom. The electron mechanism of this effect is analogous to the electron mechanism of the weakening of σ bonds in the intermolecular interactions upon increase of their polarity (cf. the second Gutmann's rule³⁹): the increase of the polarity of a covalent bond decreases the resonance contribution to the bond energy. The consideration of the π polarization of the C≡N bond, besides the σ donation from the nitrogen lone pair (see Introduction), can explain the found closeness of the $\Delta\nu(\text{CN})$ shifts of CD₃CN on Mg_{3c} and Mg_{4c} sites: on going from Mg_{4c} to Mg_{3c} the strengthening of the C≡N bond due to the stabilization of the σ orbital is compensated by its weakening due to the destabilization of the π orbitals. This can also explain why a similar effect does not take place for the $\nu(\text{CO})$ frequency of CO on these sites⁴ and why the $\Delta\nu(\text{CO})$ shifts of CO upon adsorption^{4,40-42} are larger than the $\Delta\nu(\text{CN})$ shifts of CD₃CN on the same sites^{15-17,19} in most cases: as CO coordinates on electron-acceptor sites exclusively by the C end, i.e., by the less electronegative atom of the multiple bond, both the σ donation from the lone pair and the polarization of the π orbitals should strengthen the C=O bond.^{20,37,38} To illustrate this difference between CD₃CN and CO probe molecules and the reliability of the theoretical approach used as well, in Table 4 we report the experimental and calculated $\Delta\nu(\text{CN})$ and $\Delta\nu(\text{CO})$ shifts of CD₃CN and CO on acidic sites of oxides.

The data of Table 4 suggest also a further detail of the mutual compensation of the σ donation and π polarization effects on

TABLE 4: $\Delta\nu(\text{CN})$ and $\Delta\nu(\text{CO})$ Frequency Shifts of CO and CD₃CN (cm⁻¹)

surface site	molecular model	$\Delta\nu(\text{CN})^a$		$\Delta\nu(\text{CO})^b$	
		exp	calcd ^c	exp	calcd ^c
≡Si-OH	Si(OH) ₄	6 ^{d,e}	7 ^f	15 ^g	21 ^f
≡P-OH	OP(OH) ₃	(?)	10	29 ^h	29 ^f
Mg _{3c}	Mg ₄ O ₄	30	26	59 ⁱ	58 ^f
Mg _{4c}	Mg ₆ O ₆	21	24	16 ⁱ	20 ^f
Al _{3c}	Al(OH) ₃	60 ^{e,j}	63 ^f	87 ^{g,k}	89 ^f
Al _{5c}	Al(OH) ₃ ·2H ₂ O	51 ^e		57 ^{g,k}	

^a With respect to free CD₃CN experimental $\nu(\text{CN}) = 2272$ cm⁻¹ and calculated $\nu(\text{CN}) = 2623$ cm⁻¹ frequencies. ^b With respect to free CO experimental $\nu(\text{CO}) = 2143$ cm⁻¹ and calculated $\nu(\text{CO}) = 2439$ cm⁻¹ frequencies. ^c 6-31G* basis set. ^d Reference 16. ^e Reference 19. ^f Reference 26. ^g Reference 41. ^h Reference 40. ⁱ Reference 4. ^j References 15 and 17. ^k Reference 42.

the C≡N bond. On increasing the acidity in series of structurally related Lewis adsorbing sites, the $\Delta\nu(\text{CN})$ increases noticeably (cf. the change of the $\Delta\nu(\text{CN})$ shift on going from a Mg_{3c} to a Al_{3c} site). This means that upon such an increase of the acidity the increasing stabilization of the σ orbital offsets the increasing destabilization of the π orbitals (see also ref 20). The strong reciprocal compensation of these two contributions to the $\Delta\nu(\text{CN})$ takes place only on increasing the acidity of the adsorbing Lewis site by the decrease of the coordination number of the electron-acceptor atom (cf. the change of the $\Delta\nu(\text{CN})$ on going from Mg_{4c} to Mg_{3c} and from Al_{5c} to Al_{3c} adsorbing sites). We explain this fact by a strong extra polarization effect on the π orbitals upon such structural changes, accounted for by a decrease of the screening effect on the adsorbing cation from the nearby O²⁻ surface anions. For example, on going from Mg_{4c} to Mg_{3c} the decrease of the number of the nearby O²⁻ anions causes a destabilization of the π orbitals, which compensates the stabilization of the σ orbitals due to the increase of the Lewis acidity of the adsorbing site. On changing the acidity in the series of structurally related Lewis sites,²⁰⁻²⁴ for example on going from a Mg_{3c} to a Al_{3c} site, this destabilization effect does not take place as the screening effect on the adsorbing cation from the surrounding O²⁻ is approximately constant.

2.3. CD₃CN Coordination on Multiple Mg Sites. To summarize the above discussion, the heavily overlapped $\nu(\text{CN})$ bands at 2302 and 2293 cm⁻¹ have been assigned to the CD₃CN species on Mg_{3c} and Mg_{4c} single sites at the intersections of the regular MgO faces. We have also proposed that the adsorption on Mg_{5c} single sites of the (001) faces is energetically unfavorable in comparison with the CD₃CN liquefaction.

The origin of the remaining weak bands at 2317 and 2280 cm⁻¹ has now to be investigated, and the possibility that they are associated with more complex multiple adsorbing sites should be considered. On the basis of the previous proposals on the structure of these sites by Coluccia et al.^{2,7} and by Bensitel et al.,⁶ the hypothetical CD₃CN complexes with double-Mg_{4c} and triple-Mg_{3c} sites on (110) and (111) defect faces were checked against the experimental 45 and 8 cm⁻¹ shifts of the 2317 and 2280 cm⁻¹ bands.

The predicted $\Delta\nu(\text{CN}) = 42$ cm⁻¹ shift of CD₃CN on double-Mg_{4c} sites (Figure 5, model **3a**) is in very good agreement with the experimental $\Delta\nu(\text{CN}) = 45$ cm⁻¹ shift of the 2317 cm⁻¹ band. As to CD₃CN on triple-Mg_{3c} sites (Figure 5, model **3b**), the calculations suggest that the $\nu(\text{CN})$ band of this species should be at approximately 2245 cm⁻¹, but no $\nu(\text{CN})$ band of strongly bonded CD₃CN species was observed at such low frequencies. Therefore, we conclude that the 2317 cm⁻¹ band is produced by CD₃CN species on double-Mg_{4c} sites, while the

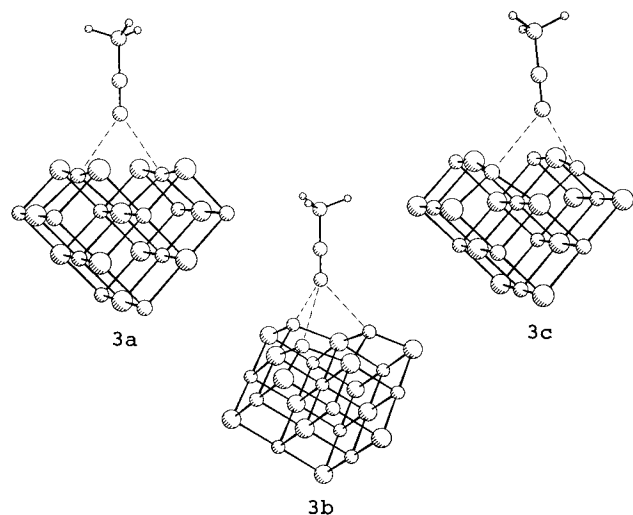
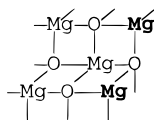


Figure 5. Molecular models of CD_3CN on double- Mg_{4c} (3a), triple- Mg_{3c} (3b), and double- Mg_{3c} (3c) sites.

surface concentration of triple- Mg_{3c} sites should be very small. This conforms to the general rule of inorganic chemistry that the larger the Miller indices of a crystal plane, the smaller the probability of its exposition. As to the negative value of the $\Delta\nu(\text{CN})$ shift on triple- Mg_{3c} sites, it can be explained by the significant deviation of the $\text{C}\equiv\text{N}\cdots\text{Mg}$ fragment from linearity in these complexes ($\angle\text{CNMg} = 139^\circ$). This geometry should result in a strong hindrance to the σ donation: the stabilization of the σ orbital cannot compensate for the destabilization of the $\text{CN } \pi$ orbitals in this case. Also, the $\text{C}\equiv\text{N}\cdots\text{Mg}$ fragment of CD_3CN on double- Mg_{4c} strongly deviates from linearity ($\angle\text{CNMg} = 144^\circ$). However, in the latter case the destabilization of the π orbitals is much less, owing to the stronger screening effect on the Mg^{2+} cations from the surrounding O^{2-} anions (see above).

According to the calculated results, neither double- Mg_{4c} nor triple- Mg_{3c} sites can be invoked in the formation of CD_3CN species responsible for the 2280 cm^{-1} band. Therefore, other multiple sites, which have not been explicitly described so far,^{2,5-7} were considered. Following the generally accepted empirical rule that the concentration of surface sites of crystals should decrease in the series surface sites on the most exposed planes > surface sites on the edges formed by the crossing of these planes > surface sites on the corners formed by the crossing of these planes, we supposed that CD_3CN on double- Mg_{3c} sites



at the intersections of the (001) and (110) faces might be responsible for the 2280 cm^{-1} band. Indeed, our computed $\Delta\nu(\text{CN}) = 4\text{ cm}^{-1}$ shift of this species (Figure 4, model 3c) is very close to the experimental $\Delta\nu(\text{CN}) = 8\text{ cm}^{-1}$ shift of the 2280 cm^{-1} band. Therefore, we assign this band to CD_3CN on double- Mg_{3c} sites. The calculated $E_{\text{bin}} = 113\text{ kJ/mol}$ of CD_3CN on double- Mg_{3c} sites agrees with the strong resistance of the 2280 cm^{-1} band upon outgassing. It is interesting to note that on going from the Mg_{4c} to the Mg_{3c} adsorbing site the $\nu(\text{CN})$ shifts by 9 cm^{-1} to higher frequencies, while on going from the double- Mg_{4c} to the double- Mg_{3c} site the $\nu(\text{CN})$ undergoes a 22 cm^{-1} shift to lower frequencies. By analogy with the mechanism of the downward $\Delta\nu(\text{CN})$ shift of CD_3CN on triple-

Mg_{3c} sites, this fact can be explained by the strong hindrance to the $\text{CD}_3\text{CN } \sigma$ donation on the multiple Mg sites due to the significant deviation of the $\text{C}\equiv\text{N}\cdots\text{Mg}$ fragment from linearity: on going from the double- Mg_{4c} to the double- Mg_{3c} adsorbing site the stabilization of the σ orbitals by the increase of the Lewis acidity cannot compensate for the destabilization of the π orbitals owing to the decrease of the screening effect on the Mg^{2+} cations from the neighboring O^{2-} anions (see above).

Conclusion

Our combined IR and quantum chemical study using CD_3CN as a molecular probe suggests multiple Mg sites of MgO ex-hydroxide to be mainly represented by double- Mg_{4c} sites on (110) defect faces and by double- Mg_{3c} sites at the intersections of the (001) and (110) faces. CD_3CN complexes with these sites manifest themselves by the $\nu(\text{CN})$ bands at 2317 and 2280 cm^{-1} . Two other $\nu(\text{CN})$ bands of coordinated CD_3CN species at 2302 and 2293 cm^{-1} are attributed to CD_3CN on Mg_{3c} and Mg_{4c} single sites of the corners and edges, respectively, at the intersections of the (001) faces. No $\nu(\text{CN})$ band is found to be associated with CD_3CN on Mg_{5c} sites of the (001) faces. The suggestion is made that the energy of adsorption on these sites should be smaller than the energy of CD_3CN liquefaction.

In our present study, among all the experimental IR data on the CD_3CN adsorption on MgO ex-hydroxide, only the $\Delta\nu(\text{CN})$ frequency shift of coordinated CD_3CN species was analyzed. This allowed to discuss the structure of adsorbing sites and coordinated CD_3CN species. As to the chemical activity of MgO ex-hydroxide, the CD_3CN coordination is followed by its irreversible transformation, which mainly occurs on double- Mg_{4c} sites at the initial stages. The description of these products, which are associated with very intense IR bands in the $2200\text{--}1440\text{ cm}^{-1}$ region (see also ref 43), will be the subject of a separate IR and quantum chemical joint study.

Acknowledgment. A.G.P. gratefully acknowledges a fellowship from "Fondazione Antonio Ratti" (Como). E.A.P. thanks ASP (Associazione per lo Sviluppo Scientifico e Tecnologico del Piemonte). Partial support of this research by the Progetto Finalizzato "Chimica Fine" of the Italian CNR is also gratefully acknowledged.

References and Notes

- (1) Coluccia, S.; Tench, A. J. In *Proceedings of the 7th International Congress on Catalysis*; Kodansha Ltd.: Tokyo, 1980, p 1154.
- (2) Coluccia, S.; Boccuzzi, F.; Ghiotti, G.; Morterra, C. *J. Chem. Soc., Faraday Trans. 1* **1982**, 78, 2111.
- (3) Coluccia, S.; Lavagnino, S.; Marchese, L. *Mater. Chem. Phys.* **1988**, 18, 445.
- (4) Coluccia, S.; Baricco, M.; Marchese, L.; Martra, G.; Zecchina, A. *Spectrochim. Acta* **1993**, 49A, 1289.
- (5) Knözinger, E.; Jacob, K.-H.; Hofmann, P. *J. Chem. Soc., Faraday Trans. 1993*, 89 (7), 1101.
- (6) Bensitel, M.; Saur, O.; Lavalley, J. C. *Mater. Chem. Phys.* **1991**, 28, 309.
- (7) Coluccia, S.; Boccuzzi, F.; Ghiotti, G.; Mirra, C. *Z. Phys. Chem. (Munich)* **1980**, 121, 141.
- (8) Anchell, J. L.; Morokuma, K.; Hess, A. C. *J. Chem. Phys.* **1993**, 99, 6004.
- (9) Kobayashi, H.; Yamaguchi, M. *J. Phys. Chem.* **1990**, 94, 7206.
- (10) Kobayashi, H.; Salahub, D. R.; Ito, T. *Catal. Today* **1995**, 23, 357.
- (11) Pacchioni, G.; Minerva, T.; Bagus, P. S. *Surf. Sci.* **1992**, 275, 450.
- (12) Neyman, K. M.; Rösch, N. *Surf. Sci.* **1993**, 297, 223.
- (13) Sawabe, K.; Koga, N.; Morokuma, K.; Iwasawa, Y. *J. Chem. Phys.* **1992**, 97, 6871.
- (14) Sauer, J.; Ugliengo, P.; Garrone, E.; Saunders, V. R. *Chem. Rev.* **1994**, 94, 2095 and references therein.
- (15) Rouxhet, P. G.; Sempels, R. E. *J. Chem. Soc., Faraday Trans. 1* **1974**, 70, 2021.
- (16) Scokart, P. O.; Declerck, F. D.; Sempels, R. E.; Rouxhet, P. G. *J. Chem. Soc., Faraday Trans. 1* **1977**, 73, 359.

- (17) Sempels, R. E.; Rouxhet, P. G. *J. Colloid. Interface Sci.* **1976**, *55*, 263.
- (18) Angell, C. L.; Howell, M. V. *J. Phys. Chem.* **1969**, *73*, 2551.
- (19) Pelmeshchikov, A. G.; van Santen, R. A.; Janchen, J.; Meijer, E. *J. Phys. Chem.* **1993**, *97*, 11071.
- (20) Purcell, K. F.; Drago, R. S. *J. Am. Chem. Soc.* **1966**, *88*, 919.
- (21) Terenin, A.; Filimonov, V.; Bistrov, D. Z. *Elektrochem.* **1958**, *62*, 180.
- (22) Filimonov, V. N.; Bistrov, D. S. *Opt. Spectrosc.* **1962**, *12*, 31.
- (23) Purcell, K. F. *J. Am. Chem. Soc.* **1967**, *89*, 247.
- (24) Purcell, K. F. *J. Am. Chem. Soc.* **1967**, *89*, 6139.
- (25) Venkateswarlu, P. *J. Chem. Phys.* **1951**, *19*, 293.
- (26) Pelmeshchikov, A. G.; Morosi, G.; Gamba, A.; Coluccia, S. *J. Phys. Chem.* **1995**, *99*, 15018.
- (27) Pelmeshchikov, A. G.; Morosi, G.; Gamba, A. *J. Phys. Chem.* **1991**, *95*, 10037.
- (28) Pelmeshchikov, A. G.; Morosi, G.; Gamba, A. *J. Phys. Chem.* **1992**, *96*, 2241.
- (29) Pelmeshchikov, A. G.; Morosi, G.; Gamba, A. *J. Phys. Chem.* **1992**, *96*, 7422.
- (30) Pelmeshchikov, A. G.; Morosi, G.; Gamba, A.; Zecchina, A.; Bordiga, S.; Paukshtis, E. A. *J. Phys. Chem.* **1993**, *97*, 11979.
- (31) Pelmeshchikov, A. G.; van Santen, R. A. *J. Phys. Chem.* **1993**, *97*, 10678.
- (32) Frisch, M. J.; Trucks, G. W.; Head-Gordon, M.; Gill, P. M. W.; Wong, M. W.; Foresman, J. B.; Johnson, B. G.; Schlegel, H. B.; Robb, M. A.; Replogle, E. S.; Gomperts, R.; Andres, J. L.; Raghavachari, K.; Binkley, J. S.; Gonzalez, C.; Martin, R. L.; Fox, D. J.; Defrees, D. J.; Baker, J.; Stewart, J. J. P.; Pople, J. A., Gaussian 92, Revision, 1992.
- (33) Boys, S. F.; Bernardi, F. *Mol. Phys.* **1970**, *19*, 553.
- (34) Pelmeshchikov, A. G.; Morosi, G.; Gamba, A.; Coluccia, S.; Martra, G.; Paukshtis, E. To be published.
- (35) Scamehorn, C. A.; Hess, A. C.; McCarthy, M. I. *J. Chem. Phys.* **1993**, *99* (4), 2786.
- (36) For comparison, the related shift of the $\nu(\text{CO})$ frequency of CO is 43 cm^{-1} .
- (37) Cotton, F. A.; Barnes, R. D.; Bannister, E. *J. Chem. Soc.* **1960**, 2139.
- (38) Brown, T. L.; Kubota, M. *J. Am. Chem. Soc.* **1961**, *83*, 4175.
- (39) Gutmann, V. *The Donor-Acceptor Approach to Molecular Interactions*; Plenum Press: New York, 1978.
- (40) Kikhtianin, O. V.; Paukshtis, E. A.; Ione, K. G.; Mastikhin, V. M. *J. Catal.* **1990**, *126*, 1.
- (41) Kustov, L. M.; Kazansky, V. B.; Beran, S.; Kubelkova, L.; Jiru, P. *J. Phys. Chem.* **1987**, *91*, 5247.
- (42) Pelmeshchikov, A. G.; Paukshtis, E. A.; Stepanov, V. G.; Ione, K. G.; Zhidomirov, G. M.; Zamaraev, K. I. In *Proceedings of the 9th International Congress on Catalysis*, Calgary, Canada, 1987; Vol. 1, p 404.
- (43) Koubowetz, F.; Latzel, J.; Noller, H. *J. Colloid Interf. Sci.* **1980**, *74*, 322.

JP952720B